Available online at www.sciencedirect.com

ScienceDirect

IFAC PapersOnLine 50-1 (2017) 6029–6034

Control design for a pneumatic isolation table including different time delays dependent on control input polarity

Satoshi Kumata * Kenta Narumi * Tomoharu Iida * Naoto Maruyama * Masaya Tanemura ** Yuichi Chida ***

* *Graduate School of Science and Technology, Shinshu University, Nagano, Japan.*
** *Interdisciplinary Graduate School of Science and Technology, Shinshu University, Nagano, Japan.*
*** *Faculty of Engineering, Shinshu University, Nagano, Japan (e-mail: chida@shinshu-u.ac.jp)*

Abstract: In the present paper, we discuss control design for a pneumatic isolation table including different time delays that are dependent on control input polarity. For such a plant, the control design problem is essentially that for a switched system. In the present paper, we first describe a model of the plant. The plant is represented by a linear system in which the input matrix in the state-space representation changes depending on the input polarity. Next, we discuss state-feedback control design for the system. A controller is obtained by solving an optimal problem, which guarantees stability as well as control performance, using linear matrix inequality (LMI) techniques. Finally, the control performance achieved by the proposed method is verified through numerical simulations.

Keywords: input time delay, pneumatic isolation table, vibration control, switched system, state feedback control

1. INTRODUCTION

Pneumatic isolation tables are used in numerous manufacturing fields, and active controls are used to apply appropriate damping effects to the tables (T.Kato et al. (2010, 2007)). In the present paper, we discuss control design for a pneumatic isolation table, including time delays of different lengths depending on control input polarity. The control input for the table is generated by driving air inflow valves from pressure tanks to air springs or by driving air exhaust valves from the springs to atmospheric air. The length of the transport route of air and the performances of the valves produce an input time delay to a plant and differ between inflow and exhaust devices. Therefore, the plant includes different time delays depending on input polarity. For such a plant, the control design problem is essentially that for a switched system. In the present paper, we first describe a model of the plant. The model is represented as a linear system, the input matrix in the state-space representation of which changes depending on the input polarity. In contrast, the state variables and the coefficient matrix of the state are the same if the input polarity changes. Next, we discuss state feedback control design for the system. Since the system consists of two different control input structures depending on the polarity of the input, two state feedback gains are designed for each control input structure and are switched depending on the state variable. The feedback gains are designed such that they guarantee the stability of the system if the control is switched. A controller is obtained by solving an optimal problem, which guarantees the stability of the switching control. The stability is guaranteed based on the Lyapunov method by using linear matrix inequalities (LMIs). Finally, the control performance for a pneumatic isolation table system provided by the proposed method is verified through numerical simulations. The effectiveness of the designed control gains and switching control law is shown. A number of studies have investigated control for a pneumatic isolation table (M.Koike et al. (2013); N.Maruyama et al. (2015); T.Kato et al. (2007); J.Sun and K.Kim (2013); M. Heertjes (2006); K.Kawashima et al. (2007)) and time-delay control (Y.H.Shin and K.J.Kim (2009); P.Chang et al. (2010)). However, to our knowledge, there has been no investigation of a control problem considering differences in input time delays depending on the input polarity. On the other hand, a number of studies have examined control problems of time-delay systems using the H_∞ loop shaping method or the classical Smith compensation (A.Kojima and Y.Ichikawa (2008)). Moreover, X.Dongmei et al. (2008) discussed control synthesis for a switched system with input time delay. However, they assumed a single time delay in each control input channel, and their control cannot be applied to a system that includes different time delays depending on the polarity of the input. Thus, control design for the switched system considered herein has not yet been reported.

⋆ Sponsor and financial support acknowledgment goes here. Paper titles should be written in uppercase and lowercase letters, not all uppercase.

2405-8963
Peer review under responsibility of International Federation of Automatic Control.
10.1016/j.ifacol.2017.08.1443

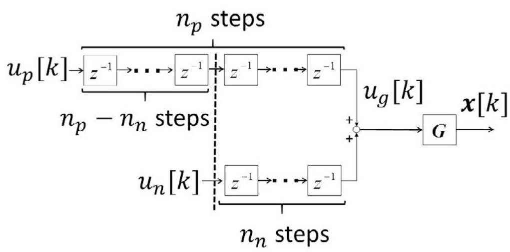

Fig. 1. Block diagram of the plant

In the present paper, $\mathbb{R}$ and $\mathbb{N}_+$ denote the set of real numbers and the set of positive integers, respectively, and $\boldsymbol{I}$ and $\mathbf{0}_{n\times m}$ represent the unity matrix and a zero matrix of size $n \times m$, respectively.

2. CONTROLLED SYSTEM

2.1 Plant

The controlled system given by the following equation is discussed in the present paper:

$$G : \boldsymbol{x}[k+1] = \boldsymbol{A}\boldsymbol{x}[k] + \boldsymbol{b}u_g[k] \qquad (1)$$
$$u_g[k] = u_p[k-n_p] + u_n[k-n_n]$$

where $\boldsymbol{x}[k] \in \mathbb{R}^{\,n_g\times 1}$ is the state vector and is assumed to be measurable, $u_g[k] \in \mathbb{R}^1$ is the control input, and $\boldsymbol{A}$ and $\boldsymbol{b}$ are a constant matrix and a vector, respectively. It is assumed that $(\boldsymbol{A},\ \boldsymbol{b})$ is controllable. Where, n_u and n_s are defined as $n_u = \max(n_p, n_n)$ and $n_s = n_g + n_u$. The control input $u_g[k]$ consists of a positive value input, $u_p[k] \in \mathbb{R}^1$, and a negative value input, $u_n[k] \in \mathbb{R}^1$. These two inputs are applied to G with different input time delays. The time delay for a positive input is $n_p \in \mathbb{N}_+$, and that for a negative input is $n_n \in \mathbb{N}_+$. It is assumed that $n_p > n_n$ and $n_u = n_p$ for the convenience of the present paper, but the discussion of the paper can be applied to the case of $n_p < n_n$ and $n_u = n_n$. We assume that the inputs of the positive input $u_p[k]$ and the negative input $u_n[k]$ cannot be simultaneously added to the system, which is therefore considered to be a switched system depending on the polarity of the control inputs. A block diagram of the system is shown in Fig. 1. The system appears in a control problem of a pneumatic isolation table, and an example model is shown in Section 5.

2.2 State-space Model

The controlled system in Fig. 1 can be transformed to the system shown in Fig. 2 by equivalent transformation. Two inputs cannot be added to the system simultaneously. As such, the system cannot be considered to be a two-input system, but is instead considered to be an input-switched system depending on the polarity of the input. Thus, the two systems shown in Fig. 3 and Fig. 4 are switched depending on the sign of the input, $u_p[k]$ or $u_n[k]$. The state-space representation of the equivalent system is described as follows:

$$\tilde{G} : \tilde{\boldsymbol{x}}[k+1] = \tilde{\boldsymbol{A}}\tilde{\boldsymbol{x}}[k] + \boldsymbol{\alpha}[k] \qquad (2)$$

$$\boldsymbol{\alpha}[k] = \tilde{\boldsymbol{b}}_p u_p[k] \text{ or } \boldsymbol{\alpha}[k] = \tilde{\boldsymbol{b}}_n u_n[k] \qquad (3)$$

Where,

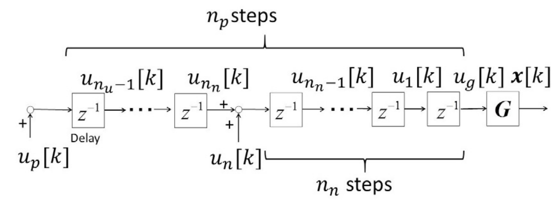

Fig. 2. Equivalent system of the plant

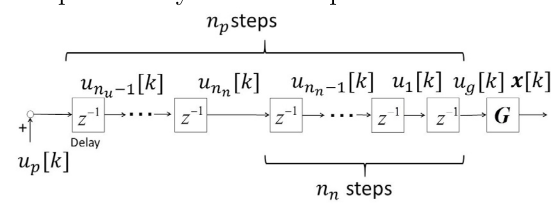

Fig. 3. Block diagram in the case of a positive input

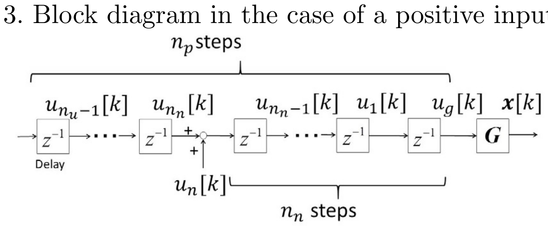

Fig. 4. Block diagram in the case of a negative input

$$\tilde{\boldsymbol{x}}[k] = \left[\begin{array}{c} \boldsymbol{x}[k] \\ \hline u_g[k] \\ u_1[k] \\ \vdots \\ u_{n_n-2}[k] \\ u_{n_n-1}[k] \\ \hline u_{n_n}[k] \\ u_{n_n+1}[k] \\ \vdots \\ u_{n_u-2}[k] \\ \hline u_{n_u-1}[k] \end{array}\right],\ \tilde{\boldsymbol{b}}_p = \left[\begin{array}{c} \mathbf{0} \\ \hline 0 \\ 0 \\ \vdots \\ 0 \\ 0 \\ \hline 0 \\ 0 \\ \vdots \\ 0 \\ \hline 1 \end{array}\right],\ \tilde{\boldsymbol{b}}_n = \left[\begin{array}{c} \mathbf{0} \\ \hline 0 \\ 0 \\ \vdots \\ 0 \\ 1 \\ \hline 0 \\ 0 \\ \vdots \\ 0 \\ \hline 0 \end{array}\right] \qquad (4)$$

$$\tilde{\boldsymbol{A}} = \left[\begin{array}{c|c|cccc|c} \boldsymbol{A} & \boldsymbol{b} & & \mathbf{0} & & & \mathbf{0} \\ \hline & & 1 & 0 & \cdots & & 0 \\ & & 0 & 1 & & & \\ & & & & 1 & & \\ \mathbf{0} & \mathbf{0} & \vdots & & \ddots & & \vdots \\ & & & & & 1 & \\ & & & & & & 1 \\ \hline & & & & & & 1 \\ \mathbf{0} & \mathbf{0} & 0 & & \cdots & & 1 \\ \hline 0 & 0 & 0 & & \cdots & & 0 \end{array}\right] \qquad (5)$$

The state vector $\tilde{\boldsymbol{x}}[k]$ is assumed to be measurable. Note that $\tilde{\boldsymbol{b}}_p$ and $\tilde{\boldsymbol{b}}_n$ differ depending on the length of the input time delay, and the input is added to the system through different input vectors. Therefore, the system is considered to be a switched system. In contrast, the state vector $\tilde{\boldsymbol{x}}[k]$ and the coefficient matrix $\tilde{\boldsymbol{A}}$ are invariant for the switched input. Although $(\tilde{\boldsymbol{A}},\ \tilde{\boldsymbol{b}}_p)$ is controllable, $(\tilde{\boldsymbol{A}},\ \tilde{\boldsymbol{b}}_n)$ is not controllable, because it includes $n_u - n_n$ of uncontrollable z^{-1}. Moreover, z^{-1} is stable, so $(\tilde{\boldsymbol{A}},\ \tilde{\boldsymbol{b}}_n)$ is stabilizable.

3. CONTROL LAW

The regulation problem using the state feedback control is considered in the present paper. Since the inputs differ according to the polarity of them and cannot be added to the system simultaneously, $u_p[k]$ and $u_n[k]$ are switched by an appropriate control law. The following control law is adopted in the present paper. First, two feedback control gains, $\boldsymbol{F}_p$ and $\boldsymbol{F}_n$, are appropriately designed in the proposed procedure such that the absolute values of all of the eigenvalues of $\tilde{\boldsymbol{A}} - \tilde{\boldsymbol{b}}_p\boldsymbol{F}_p$, $\tilde{\boldsymbol{A}} - \tilde{\boldsymbol{b}}_n\boldsymbol{F}_n$, and $\tilde{\boldsymbol{A}} - \tilde{\boldsymbol{b}}_p\boldsymbol{F}_n$ are less than 1 and the stability of the system by switching of the input is guaranteed. In order to guarantee the stability of switching control, feedback gains $\boldsymbol{F}_p$ and $\boldsymbol{F}_n$ are designed such that the following inequalities are satisfied:

$$\begin{cases} (\tilde{\boldsymbol{A}} - \tilde{\boldsymbol{b}}_p\boldsymbol{F}_p)^{\mathrm{T}}\boldsymbol{P}(\tilde{\boldsymbol{A}} - \tilde{\boldsymbol{b}}_p\boldsymbol{F}_p) - \boldsymbol{P} < 0 \\ (\tilde{\boldsymbol{A}} - \tilde{\boldsymbol{b}}_n\boldsymbol{F}_n)^{\mathrm{T}}\boldsymbol{P}(\tilde{\boldsymbol{A}} - \tilde{\boldsymbol{b}}_n\boldsymbol{F}_n) - \boldsymbol{P} < 0 \\ (\tilde{\boldsymbol{A}} - \tilde{\boldsymbol{b}}_p\boldsymbol{F}_n)^{\mathrm{T}}\boldsymbol{P}(\tilde{\boldsymbol{A}} - \tilde{\boldsymbol{b}}_p\boldsymbol{F}_n) - \boldsymbol{P} < 0 \\ \boldsymbol{P} > 0 \end{cases} \quad (6)$$

This requires the existence of a common solution of $\boldsymbol{P} > 0$ (T.Iida and Y.Chida (2014)). It is assumed the $\boldsymbol{P} > 0$ exists. As shown in the next section, control design is executed using LMIs. In the control design procedure, $\boldsymbol{F}_p$ and $\boldsymbol{F}_n$ are selected such that they provide sufficient control performance for $u_p[k] = -\boldsymbol{F}_p\tilde{\boldsymbol{x}}[k]$ and $u_n[k] = -\boldsymbol{F}_n\tilde{\boldsymbol{x}}[k]$, respectively. Note that the second inequality in (6) guarantees the stability even if $(\tilde{\boldsymbol{A}},\ \tilde{\boldsymbol{b}}_n)$ is uncontrollable.

Second, the control input is selected according to the following switching law: $\Psi(\tilde{\boldsymbol{x}}[k])$,

$$\Psi(\tilde{\boldsymbol{x}}[k]) = \begin{cases} \text{(i)} : u_p[k] = -\boldsymbol{F}_p\tilde{\boldsymbol{x}}[k],\quad u_n[k] = 0 \\ \qquad \text{if } -\boldsymbol{F}_p\tilde{\boldsymbol{x}}[k] > 0 \wedge -\boldsymbol{F}_n\tilde{\boldsymbol{x}}[k] > 0 \\ \text{(ii)} : u_p[k] = 0,\quad u_n[k] = -\boldsymbol{F}_n\tilde{\boldsymbol{x}}[k] \\ \qquad \text{if } -\boldsymbol{F}_p\tilde{\boldsymbol{x}}[k] < 0 \wedge -\boldsymbol{F}_n\tilde{\boldsymbol{x}}[k] < 0 \\ \text{(iii)} : u_p[k] = 0,\quad u_n[k] = -\boldsymbol{F}_n\tilde{\boldsymbol{x}}[k] \\ \qquad \text{if } -\boldsymbol{F}_p\tilde{\boldsymbol{x}}[k] > 0 \wedge -\boldsymbol{F}_n\tilde{\boldsymbol{x}}[k] < 0 \\ \text{(iv)} : u_p[k] = -\boldsymbol{F}_n\tilde{\boldsymbol{x}}[k],\quad u_n[k] = 0 \\ \qquad \text{if } -\boldsymbol{F}_p\tilde{\boldsymbol{x}}[k] < 0 \wedge -\boldsymbol{F}_n\tilde{\boldsymbol{x}}[k] > 0 \\ \text{(v)} : u_p[k] = 0,\quad u_n[k] = 0 \\ \qquad \text{if } -\boldsymbol{F}_p\tilde{\boldsymbol{x}}[k] = 0 \wedge -\boldsymbol{F}_n\tilde{\boldsymbol{x}}[k] = 0 \end{cases} \quad (7)$$

In case (i), both $-\boldsymbol{F}_p\tilde{\boldsymbol{x}}[k]$ and $-\boldsymbol{F}_n\tilde{\boldsymbol{x}}[k]$ are positive. In this case, $u_p[k] = -\boldsymbol{F}_p\tilde{\boldsymbol{x}}[k]$ is selected because $\boldsymbol{F}_p$ is designed such that $u_p[k] = -\boldsymbol{F}_p\tilde{\boldsymbol{x}}[k]$ provides sufficient control performance. In case (ii), both $-\boldsymbol{F}_p\tilde{\boldsymbol{x}}[k]$ and $-\boldsymbol{F}_n\tilde{\boldsymbol{x}}[k]$ are negative. In this case, $u_n[k] = -\boldsymbol{F}_n\tilde{\boldsymbol{x}}[k]$ is selected because $\boldsymbol{F}_n$ is designed such that $u_n[k] = -\boldsymbol{F}_n\tilde{\boldsymbol{x}}[k]$ provides sufficient control performance. In contrast, several selectable combinations exist in cases (iii) and (iv). In the present paper, for the sake of convenience, $\boldsymbol{F}_n$ is selected for cases (iii) and (iv). The first reason for this selection is that $\boldsymbol{F}_n$ is an appropriate gain for $\tilde{\boldsymbol{b}}_n$, the time delay of which is shorter than $\tilde{\boldsymbol{b}}_p$. The second reason for this selection is that it is possible to reduce the conservativeness. That is, the minimum number of Lyapunov inequalities in (6) for the switching is considered. A flowchart of the control input decision procedure is shown in Fig. 5. A block diagram

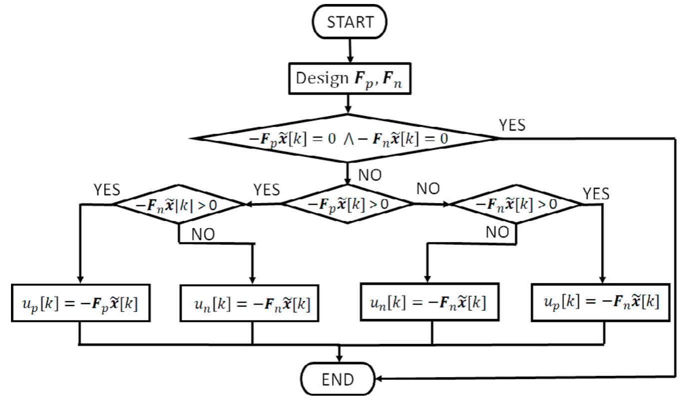

Fig. 5. Flow chart of the proposed input switching

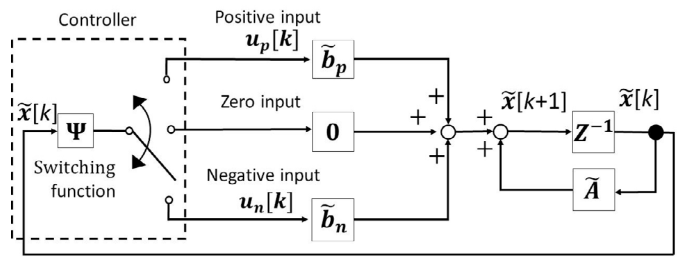

Fig. 6. Block diagram of the proposed switched system

of the control system using the switching control law is shown in Fig. 6.

4. DESIGN OF FEEDBACK GAIN

4.1 Problem Statement

In this section, feedback gains $\boldsymbol{F}_p$ and $\boldsymbol{F}_n$ are designed. First, we assume that reference feedback gains $\boldsymbol{F}_p^* \in \mathbb{R}^{1\times n_s}$ and $\boldsymbol{F}_n^* \in \mathbb{R}^{1\times n_s}$ are designed in advance such that $\tilde{\boldsymbol{A}} - \tilde{\boldsymbol{b}}_p\boldsymbol{F}_p^*$ and $\tilde{\boldsymbol{A}} - \tilde{\boldsymbol{b}}_n\boldsymbol{F}_n^*$ provide desired performance. Note that $\boldsymbol{F}_p^*$ and $\boldsymbol{F}_n^*$ do not necessarily satisfy (6). The design method of $\boldsymbol{F}_p^*$ and $\boldsymbol{F}_n^*$ is described in the next section. If $\boldsymbol{F}_p^*$ and $\boldsymbol{F}_n^*$ are obtained, feedback gains $\boldsymbol{F}_p$ and $\boldsymbol{F}_n$, which provide approximately the same performance for $\boldsymbol{F}_p^*$ and $\boldsymbol{F}_n^*$, are designed in the next step based on the following performance index (M.Tanemura and Y.Chida (2016)).

$$J(\boldsymbol{F}) = (\boldsymbol{F} - \boldsymbol{F}^*)\boldsymbol{M}(\boldsymbol{F} - \boldsymbol{F}^*)^{\mathrm{T}} \quad (8)$$

$$\boldsymbol{F}^* := [\boldsymbol{F}_p^*\ \ \boldsymbol{F}_n^*],\ \boldsymbol{F} := [\boldsymbol{F}_p\ \ \boldsymbol{F}_n] \quad (9)$$

$$\boldsymbol{M} := \begin{bmatrix} \boldsymbol{M}_p & \boldsymbol{0} \\ \boldsymbol{0} & \boldsymbol{M}_n \end{bmatrix} \quad (10)$$

where the reference feedback gains $\boldsymbol{F}_p^*$ and $\boldsymbol{F}_n^*$ are represented as

$$\boldsymbol{F}_p^* = [\tilde{f}_{p,1}^*,\ \tilde{f}_{p,2}^*,\ \cdots\ ,\tilde{f}_{p,n_s}^*], \quad (11)$$

$$\boldsymbol{F}_n^* = [\tilde{f}_{n,1}^*,\ \tilde{f}_{n,2}^*,\ \cdots\ ,\tilde{f}_{n,n_g+n_n}^*, \boldsymbol{0}_{1\times(n_u-n_n)}]. \quad (12)$$

Moreover, $\boldsymbol{M}_p$ and $\boldsymbol{M}_n$ are weighting matrices, which are defined as

$$\boldsymbol{M}_p := \mathrm{diag}[1/(\tilde{f}_{p,1}^*)^2, 1/(\tilde{f}_{p,2}^*)^2,\ \cdots\ ,1/(\tilde{f}_{p,n_s}^*)^2], \quad (13)$$

$$\boldsymbol{M}_n := \mathrm{diag}[1/(\tilde{f}_{n,1}^*)^2, 1/(\tilde{f}_{n,2}^*)^2,\ \cdots\ ,1/(\tilde{f}_{n,n_g+n_n}^*)^2 ,1\ ,1\ ,\ \cdots\ ,\ 1,\ 1]. \quad (14)$$

Here, $\boldsymbol{M}_p$ and $\boldsymbol{M}_n$ are specified for normalization of the error between $\boldsymbol{F}_p - \boldsymbol{F}_p^*$ and $\boldsymbol{F}_n - \boldsymbol{F}_n^*$ in $J(\boldsymbol{F})$.

Moreover, $\boldsymbol{F}_p$ and $\boldsymbol{F}_n$ are designed by minimizing $J(\boldsymbol{F})$ in (8) using $\boldsymbol{F}_p^*$ and $\boldsymbol{F}_n^*$, respectively. At the same time, the stability conditions in (6) are guaranteed. The problem to be solved is as follows:

$$\min_{\boldsymbol{F},\boldsymbol{P}} J(\boldsymbol{F}) \text{ s.t. } \begin{cases} (\tilde{\boldsymbol{A}} - \tilde{\boldsymbol{b}}_p\boldsymbol{F}_p)^{\mathrm{T}}\boldsymbol{P}(\tilde{\boldsymbol{A}} - \tilde{\boldsymbol{b}}_p\boldsymbol{F}_p) - \boldsymbol{P} < 0 \\ (\tilde{\boldsymbol{A}} - \tilde{\boldsymbol{b}}_n\boldsymbol{F}_n)^{\mathrm{T}}\boldsymbol{P}(\tilde{\boldsymbol{A}} - \tilde{\boldsymbol{b}}_n\boldsymbol{F}_n) - \boldsymbol{P} < 0 \\ (\tilde{\boldsymbol{A}} - \tilde{\boldsymbol{b}}_p\boldsymbol{F}_n)^{\mathrm{T}}\boldsymbol{P}(\tilde{\boldsymbol{A}} - \tilde{\boldsymbol{b}}_p\boldsymbol{F}_n) - \boldsymbol{P} < 0 \\ \boldsymbol{P} > 0 \end{cases} \tag{15}$$

4.2 LMI Method for Solving the Optimization Problem

The optimization problem of (15) is solved using the LMI method. Since the problem is non-convex, it is transformed to a convex problem that can be solved as an LMI formulation by using Tanemura's method (M.Tanemura and Y.Chida (2016)).

At the beginning, the stability conditions of (6) are represented as the following LMIs:

$$\begin{bmatrix} \boldsymbol{X} & \boldsymbol{A}_{pp}\boldsymbol{X} - \tilde{\boldsymbol{b}}_p\boldsymbol{y}_p^{\mathrm{T}} \\ \boldsymbol{X}\boldsymbol{A}_{pp}^{\mathrm{T}} - \boldsymbol{y}_p\tilde{\boldsymbol{b}}_p^{\mathrm{T}} & \boldsymbol{X} \end{bmatrix} > 0 \tag{16}$$

$$\begin{bmatrix} \boldsymbol{X} & \boldsymbol{A}_{nn}\boldsymbol{X} - \tilde{\boldsymbol{b}}_n\boldsymbol{y}_n^{\mathrm{T}} \\ \boldsymbol{X}\boldsymbol{A}_{nn}^{\mathrm{T}} - \boldsymbol{y}_n\tilde{\boldsymbol{b}}_n^{\mathrm{T}} & \boldsymbol{X} \end{bmatrix} > 0 \tag{17}$$

$$\begin{bmatrix} \boldsymbol{X} & \boldsymbol{A}_{pn}\boldsymbol{X} - \tilde{\boldsymbol{b}}_p\boldsymbol{y}_n^{\mathrm{T}} \\ \boldsymbol{X}\boldsymbol{A}_{pn}^{\mathrm{T}} - \boldsymbol{y}_n\tilde{\boldsymbol{b}}_p^{\mathrm{T}} & \boldsymbol{X} \end{bmatrix} > 0 \tag{18}$$

where $\boldsymbol{A}_{pp}$, $\boldsymbol{A}_{nn}$, and $\boldsymbol{A}_{pn}$ are defined as

$$\boldsymbol{A}_{pp} := (\tilde{\boldsymbol{A}} - \tilde{\boldsymbol{b}}_p\boldsymbol{F}_p^*), \tag{19}$$

$$\boldsymbol{A}_{nn} := (\tilde{\boldsymbol{A}} - \tilde{\boldsymbol{b}}_n\boldsymbol{F}_n^*), \tag{20}$$

$$\boldsymbol{A}_{pn} := (\tilde{\boldsymbol{A}} - \tilde{\boldsymbol{b}}_p\boldsymbol{F}_n^*). \tag{21}$$

and $\boldsymbol{y}_p \in \mathbb{R}^{n_s\times 1}$ and $\boldsymbol{y}_n \in \mathbb{R}^{n_s\times 1}$ are defined as

$$\boldsymbol{y}_p := \boldsymbol{X}\Delta\boldsymbol{F}_p^{\mathrm{T}}, \quad \boldsymbol{y}_n := \boldsymbol{X}\Delta\boldsymbol{F}_n^{\mathrm{T}}. \tag{22}$$

Where,$\Delta\boldsymbol{F}_p$ and $\Delta\boldsymbol{F}_n$ are defined as

$$\Delta\boldsymbol{F}_p := \boldsymbol{F}_p - \boldsymbol{F}_p^*, \quad \Delta\boldsymbol{F}_n := \boldsymbol{F}_n - \boldsymbol{F}_n^*. \tag{23}$$

Moreover, $\boldsymbol{X} \in \mathbb{R}^{n_s\times n_s}$ is defined as

$$\boldsymbol{X} := \boldsymbol{P}^{-1}. \tag{24}$$

These inequalities are convex for variables of $\boldsymbol{y}_p$, $\boldsymbol{y}_n$, and $\boldsymbol{X}$.

In order to transform the performance index of (8) to the LMI condition, γ is introduced, and the problem is described as a γ-minimization problem for $\gamma > J$. According to Tanemura (M.Tanemura and Y.Chida (2016)), the problem is described as a γ-minimization problem using the following LMIs:

$$\begin{bmatrix} \alpha\boldsymbol{X}_m & \boldsymbol{y}_m \\ \boldsymbol{y}_m^{\mathrm{T}} & \gamma \end{bmatrix} > \boldsymbol{0}, \quad \boldsymbol{X}_m > \alpha\boldsymbol{M} \tag{25}$$

where α is a constant satisfying $\alpha > 0$, and

$$\boldsymbol{X}_m := \begin{bmatrix} \boldsymbol{X} & \boldsymbol{0} \\ \boldsymbol{0} & \boldsymbol{X} \end{bmatrix}, \ \boldsymbol{y}_m := \begin{bmatrix} \boldsymbol{y}_p \\ \boldsymbol{y}_n \end{bmatrix}. \tag{26}$$

Equation (25) is a sufficient condition for $\gamma > J$ holding. Using the described transformation, the minimization problem of (15) is changed to the γ minimization problem described in the following equation:

$$\min_{\gamma,\boldsymbol{y}_m,\boldsymbol{X}_m} \gamma \ \text{ s.t. } (16),\ (17),\ (18),\ (25) \tag{27}$$

Then, the feedback gain $\boldsymbol{F} = [\boldsymbol{F}_p,\ \boldsymbol{F}_n]$ is obtained as

$$\boldsymbol{F}_p = \boldsymbol{F}_p^* + \boldsymbol{y}_p^{\mathrm{T}}\boldsymbol{X}^{-1}, \ \boldsymbol{F}_n = \boldsymbol{F}_n^* + \boldsymbol{y}_n^{\mathrm{T}}\boldsymbol{X}^{-1}. \tag{28}$$

4.3 Design of Reference Feedback Gain

The reference feedback gains $\boldsymbol{F}_p^*$ and $\boldsymbol{F}_n^*$ must be obtained in advance for the proposed procedure, and $\boldsymbol{F}_p^*$ and $\boldsymbol{F}_n^*$ are designed such that $\tilde{\boldsymbol{A}} - \tilde{\boldsymbol{b}}_p\boldsymbol{F}_p^*$ and $\tilde{\boldsymbol{A}} - \tilde{\boldsymbol{b}}_n\boldsymbol{F}_n^*$ provide the desired performances. First, a state feedback gain $\boldsymbol{F}_m \in \mathbb{R}^{1\times n_g}$ is designed by an appropriate method, such as LQ optimal control using (1), so that $\boldsymbol{A} - \boldsymbol{b}\boldsymbol{F}_m$ is stable and the eigenvalues provide sufficient convergence.

Next, $\boldsymbol{F}_p^*$ and $\hat{\boldsymbol{F}}_n^*$ are obtained by the state predictive control as

$$\boldsymbol{F}_p^* = \boldsymbol{F}_m \left[\boldsymbol{A}^{n_u} \ \ \boldsymbol{A}^{n_u-1}\boldsymbol{b} \ \cdots \ \boldsymbol{b}\right], \tag{29}$$

$$\hat{\boldsymbol{F}}_n^* = \boldsymbol{F}_m \left[\boldsymbol{A}^{n_n} \ \ \boldsymbol{A}^{n_n-1}\boldsymbol{b} \ \cdots \ \boldsymbol{b}\right], \tag{30}$$

where $\boldsymbol{F}_p^* \in \mathbb{R}^{1\times n_s}$ and $\hat{\boldsymbol{F}}_n^* \in \mathbb{R}^{1\times(n_g+n_n)}$ (K.Watanabe (1993)). The size of the state predictive control gain $\hat{\boldsymbol{F}}_n^*$ for the minimal-order system of Fig. 4 is not equal to that of $\tilde{\boldsymbol{x}}[k]$. Moreover, the feedback gain $\hat{\boldsymbol{F}}_n^*$ must be modified to be of the same size as the state vector $\tilde{\boldsymbol{x}}[k]$. Here, $\boldsymbol{F}_n^*$ is obtained by adding additional zeros to gains:

$$\boldsymbol{F}_n^* = \begin{bmatrix} \hat{\boldsymbol{F}}_n^* & \boldsymbol{0}_{1\times(n_u-n_n)} \end{bmatrix}. \tag{31}$$

Finally, the feedback gains are obtained by the following procedure:

[Design procedure]

Step 1
A feedback gain $\boldsymbol{F}_m$ is designed for the plant without the time delay of (1), such that $\boldsymbol{A} - \boldsymbol{b}\boldsymbol{F}_m$ is stable and provides sufficient regulation performance. It is possible to use an appropriate state feedback control design, such as the LQ optimal control, for the design of $\boldsymbol{F}_m$.

Step 2
$\boldsymbol{F}_p^*$ and $\boldsymbol{F}_n^*$ are specified by (29) and (31) based on the state predictive control.

Step 3
$\boldsymbol{F}_p$ and $\boldsymbol{F}_n$ are derived by solving the minimization problem of (27). The solution satisfies the stability conditions for the switched system.

5. PNEUMATIC ISOLATION TABLE CONTROL EXAMPLE

5.1 Pneumatic Isolation Table

The table is supported by four air springs, the pressures of which are controlled by air inflow into each spring or air outflow to the atmosphere. Air flow control is executed using servo valves and the air transmitted through air pipe arrangements. In such situations, time delays occur due to the transmission time of the air movement. Since the length of the pipe arrangement differs between the inflow and outflow paths, the length of the time delay differs between the inflow and the outflow. Therefore, the system includes time delays of different lengths, which depend on the polarity of the control input.

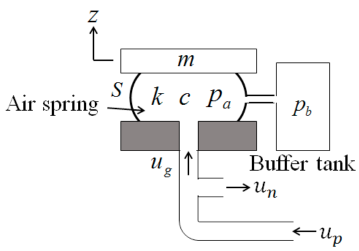

Fig. 7. Model of the pneumatic isolation table

5.2 Model

The model of the system is shown in Fig. 7. In the present paper, vertical parallel motion is considered. The control output is z, and airflow is used as the control inputs for the inflow into and the outflow from the air springs. The parameters are shown in Table 1. The motion of the table is assumed to be restricted to be parallel to the vertical motion. By considering the equilibrium condition of thermodynamics in the air springs, the equation of motion of the system is obtained as

$$m\ddot{z} + c\dot{z} + kz = Sp_a \tag{32}$$

$$\dot{p}_a = \frac{\kappa R_s T}{(z_a + hz)S}\{u_g - \mu(p_a - p_b)\} - \frac{\kappa(p_0 + p_a)}{z_a + hz}\dot{z}h \tag{33}$$

$$\dot{p}_b = \frac{\kappa R_s T}{z_b S}\mu(p_a - p_b). \tag{34}$$

If the approximation of $z_a \gg hz$ and $p_0 \gg p_a$ in (33) and (34), respectively, is executed, the state-space representation of the plant is obtained as follows:

$$\dot{\boldsymbol{x}}(t) = \boldsymbol{A}_c\boldsymbol{x}(t) + \boldsymbol{b}_c u_g(t) \tag{35}$$

where

$$\boldsymbol{x}(t) = [z \quad \dot{z} \quad p_a \quad p_b]^{\mathrm{T}} \tag{36}$$

$$\boldsymbol{A}_c = \begin{bmatrix} 0 & 1 & 0 & 0 \\ -\frac{k}{m} & -\frac{c}{m} & \frac{S}{m} & 0 \\ 0 & -\frac{\kappa}{z_a}p_0 h & -\frac{\kappa}{z_a S}R_s T\mu & \frac{\kappa}{z_a S}R_s T\mu \\ 0 & 0 & \frac{\kappa}{z_b S}R_s T\mu & -\frac{\kappa}{z_b S}R_s T\mu \end{bmatrix} \tag{37}$$

$$\boldsymbol{b}_c = \begin{bmatrix} 0 & 0 & \frac{\kappa}{z_a S}R_s T & 0 \end{bmatrix}^{\mathrm{T}}. \tag{38}$$

The system of (35) is discretized by the sampling period of T_s =2 [ms], assuming the zero-order hold. The state-space representation of the discretized model is given as

$$\boldsymbol{x}[k+1] = \boldsymbol{A}\boldsymbol{x}[k] + \boldsymbol{b}u_g[k] \tag{39}$$

As shown in Table 1, the input time delays for inflow and outflow are 20 [ms] and 10 [ms], respectively. In the discretized model, the input time delays correspond to $n_p = 10$ and $n_n = 5$ for inflow and outflow, respectively, because the sampling period is T_s =2 [ms].

5.3 Design of Feedback Gains

Feedback control gains are designed by the proposed procedure.

(Step 1) A reference feedback gain $\boldsymbol{F}_m$ is designed for the plant of (39) using the LQ optimal feedback control design. The weighting matrices for the state and the input are $\boldsymbol{Q}$ and R, respectively, and are specified as

$$\boldsymbol{Q} = \mathrm{diag}[6.5 \times 10^8 \quad 1.5 \times 10^5 \quad 1 \times 10^{-5} \quad 1 \times 10^{-5}], \tag{40}$$

$$R = 1. \tag{41}$$

Table 1. Plant parameter values

m	13.6 [kg]	Mass of table
p_0	0.035×10^6 [Pa]	Primary pressure
z_a	0.034 [m]	Equiv. air spring height
z_b	0.294 [m]	Equiv. buffer tank height
S	4.08×10^{-3} [m^2]	Contact area of air spring
T	293 [K]	Gas temperature
k	8×10^3 [N/m]	Equiv. spring constant
c	70 [Ns/m]	Equiv. damping coefficient
R_s	287 [J/(kgK)]	Gas constant
κ	1.4	Ratio of specific heat
μ	3.87×10^{-7} [kg/(sPa)]	Valve coefficient
h	0.966	Volume conversion coefficient
z	- [m]	Displacement of isolation table
p_a	- [Pa]	Air spring pressure deviation
p_b	- [Pa]	Buffer tank pressure deviation
u_g	- [kg/s]	Mass flow rate
u_p	- [kg/s]	Mass flow rate (Supply)
u_n	- [kg/s]	Mass flow rate (Exhaust)
L_p	20×10^{-3} [s]	Input time delay (Supply)
L_n	10×10^{-3} [s]	Input time delay (Exhaust)

The obtained feedback gain $\boldsymbol{F}_m$ is

$$\boldsymbol{F}_m = [4.237, \ 0.1754, \ 4.763 \times 10^{-7}, \ 4.847 \times 10^{-7}]. \tag{42}$$

(Step 2) The feedback gains of $\boldsymbol{F}_p^*$ and $\boldsymbol{F}_n^*$ are derived by (29) and (31), respectively, based on the state prediction control. The obtained gains of $\boldsymbol{F}_p^*$ and $\boldsymbol{F}_n^*$ are

$$\begin{aligned} \boldsymbol{F}_p^* = [&1.544, \ 2.074 \times 10^{-1}, \ 3.728 \times 10^{-7}, \\ &1.764 \times 10^{-6}, \ 6.212 \times 10^{-1}, \ 5.977 \times 10^{-1}, \\ &5.741 \times 10^{-1}, \ 5.508 \times 10^{-1}, \ 5.292 \times 10^{-1}, \\ &5.116 \times 10^{-1}, \ 5.029 \times 10^{-1}, \ 5.132 \times 10^{-1}, \\ &5.632 \times 10^{-1}, \ 6.959 \times 10^{-1}], \end{aligned} \tag{43}$$

$$\begin{aligned} \boldsymbol{F}_n^* = [&2.947, \ 1.985 \times 10^{-1}, \ 3.060 \times 10^{-7}, \\ &1.218 \times 10^{-6}, \ 5.116 \times 10^{-1}, \ 5.029 \times 10^{-1}, \\ &5.132 \times 10^{-1}, \ 5.632 \times 10^{-1}, \ 6.959 \times 10^{-1}, \\ &0, \ 0, \ 0, \ 0, \ 0]. \end{aligned} \tag{44}$$

(Step 3) The feedback gains of $\boldsymbol{F}_p$ and $\boldsymbol{F}_n$ are derived by solving the minimization problem described by the LMIs of (27). Here, α is specified as $\alpha = 1$. By solving the minimization problem, the obtained feedback gains are shown in the following. The minimum γ is $\gamma = 2.498$, J is $J(\boldsymbol{F}) = 0.2397$.

$$\begin{aligned} \boldsymbol{F}_p = [&1.335, \ 1.904 \times 10^{-1}, \ 3.460 \times 10^{-7}, \\ &1.651 \times 10^{-6}, \ 5.767 \times 10^{-1}, \ 5.552 \times 10^{-1}, \\ &5.333 \times 10^{-1}, \ 5.113 \times 10^{-1}, \ 4.898 \times 10^{-1}, \\ &4.702 \times 10^{-1}, \ 4.630 \times 10^{-1}, \ 4.793 \times 10^{-1}, \\ &5.390 \times 10^{-1}, \ 6.839 \times 10^{-1}] \end{aligned} \tag{45}$$

$$\begin{aligned} \boldsymbol{F}_n = [&2.298, \ 1.773 \times 10^{-1}, \ 2.860 \times 10^{-7}, \\ &1.199 \times 10^{-6}, \ 4.783 \times 10^{-1}, \ 4.691 \times 10^{-1}, \\ &4.744 \times 10^{-1}, \ 5.101 \times 10^{-1}, \ 6.092 \times 10^{-1}, \\ &-4.498 \times 10^{-3}, \ 6.361 \times 10^{-2}, \ 1.124 \times 10^{-1}, \\ &1.390 \times 10^{-1}, \ 1.435 \times 10^{-1}] \end{aligned} \tag{46}$$

6. SIMULATION RESULTS

Numerical simulations are carried out using the non-linear plant model of (32) through (34). A square-wave disturbance having a magnitude of -15 and a width of 2 [ms] is added into the acceleration term at 1 [s]

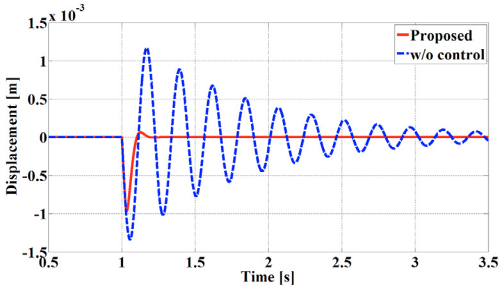

Fig. 8. Output response for a disturbance (simulation)

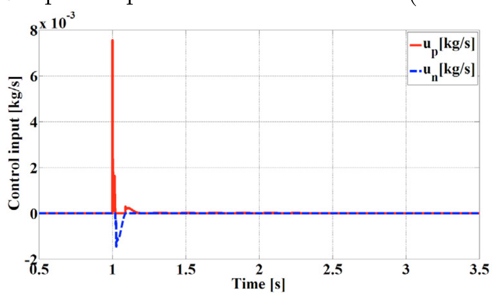

Fig. 9. Input response for a disturbance (simulation)

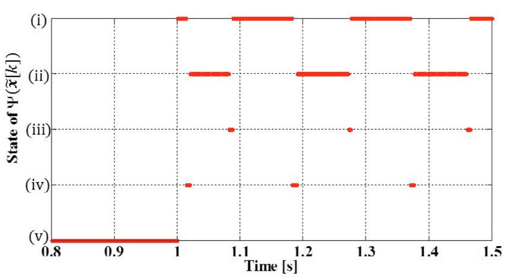

Fig. 10. States of $\Psi(\tilde{\boldsymbol{x}}[k])$ selected by the proposed procedure

after the simulation starts. The regulation performance for a disturbance by the proposed switching control is evaluated. The simulation results are shown in Fig. 8 and Fig. 9, where Fig. 8 shows the control output, which is the position of the table, z. The solid line indicates the response by the proposed switching control, and the dashed line indicates the response without control. The proposed switching control provides sufficient regulation performance. Fig. 9 shows the control input response. The control inputs for the inflow and the outflow are switched by the proposed procedure. The state of Ψ is shown in Fig. 10. As shown in the figure, the state of Ψ is appropriately selected by the proposed procedure. Almost always the states of Ψ are (i) and (ii), but (iii) and (iv) are selected in several situations. The simulation results indicate that the proposed control procedure is effective. Moreover, robustness for perturbations of time delays has been verified through numerical simulations. As a result, even if n_p and n_n vary within ±60% individually, the proposed controller maintains the control performance. Details are omitted in this paper.

7. CONCLUSIONS

We herein examined a control problem for a plant with an input time delay that varies depending on the input polarity. A state feedback control design method was proposed by solving a minimization problem, which guarantees stability for control input switching. Numerical simulations were carried out for a pneumatic isolation table model, and the results confirmed the effectiveness of the proposed method.

REFERENCES

A.Kojima and Y.Ichikawa (2008). H^∞ loop-shaping procedure for multiple input delay systems. Transactions of the Society of Instrument and Control Engineers, 44(10), 829–837.

J.Sun and K.Kim (2013). Control of transient vibrations due to stage movements in 6-dof active pneumatic table by inertial force compensation. Journal of Sound and Vibration, 332, 5241–5254.

K.Kawashima, T.Kato, K.Sawamoto, and T.Kagawa (2007). Realization of virtual sub chamber on active controlled pneumatic isolation table with pressure differentiator. Precision Engineering, 31, 139–145.

K.Watanabe (1993). Control of time-delay system. The Society of Instrument and Control Engineers.

M. Heertjes, N. (2006). Nonlinear dynamics and control of a pneumatic vibration isolator. Journal of Vibration and Acoustics, 128, 439–448.

M.Koike, Y.Chida, and Y.Ikeda (2013). Control of a pneumatic isolation table including non-linear quantizer. Transactions of the Society of Instrument and Control Engineers, 49(4), 488–496.

M.Tanemura and Y.Chida (2016). Linear matrix inequality method for a quadratic performance index minimization problem with a class of bilinear matrix inequality conditions. Journal of Physics, 744(1), 1–8. 2277.

N.Maruyama, M.Koike, and Y.Chida (2015). Model predictive control method for pneumatic isolation table with discrete-valued input. Transactions of the Society of Instrument and Control Engineers, 51(11), 755–762.

P.Chang, D.K.Han, Y.Shin, and K.Kim (2010). Effective suppression of pneumatic vibration isolators by using input-output linearization and time delay control. Journal of Sound and Vibration, 329, 1636–1652.

T.Iida and Y.Chida (2014). Feedback control design of a switched system using non-common solutions of a quadratic minimization problem. IEEE Conference on Control Applications, 1509–1514.

T.Kato, K.Kawashima, K.Sawamoto, and T.Kagawa (2007). Active control of a pneumatic isolation table using model following control and a pressure differentiator. Precision Engineering, 31, 269–275.

T.Kato, K.Kawashima, T.Funaki, K.Tadano, and T.Kagawa (2010). A new, high precision, quick response pressure regulator for active control of pneumatic vibration isolation tables. Precision Engineering, 34, 43–48.

X.Dongmei, C.Xiaoxin, and X.Ning (2008). L2 gain control synthesis of discrete-time switched systems with input time-delay. Chinese Control Conferenc, 54–57.

Y.H.Shin and K.J.Kim (2009). Performance enhancement of pneumatic vibration isolation tables in low frequency range by time delay control. Journal of Sound and Vibration, 321, 537–553.